

Decoherence and relaxation of single-electron excitations in quantum Hall edge channels

P. Degiovanni,¹ Ch. Grenier,¹ and G. Fève^{2,3}

¹Université de Lyon, Fédération de Physique André Marie Ampère, CNRS-Laboratoire de Physique de l'Ecole Normale Supérieure de Lyon, Allée d'Italie, 69364 Lyon Cedex 07, France

²Laboratoire Pierre Aigrain, Ecole Normale Supérieure, 24 rue Lhomond, 75231 Paris Cedex 05, France

³Laboratoire associé aux universités Pierre and Marie Curie et Denis Diderot, CNRS-UMR 8551, Paris, France

(Received 2 October 2009; published 11 December 2009)

A unified approach to decoherence and relaxation of energy resolved single-electron excitations in integer quantum Hall edge channels is presented. Within the bosonization framework, relaxation and decoherence induced by interactions and capacitive coupling to an external linear circuit are computed. An explicit connection with high frequency transport properties of a two terminal device formed by the edge channel on one side and the linear circuit on the other side is established.

DOI: 10.1103/PhysRevB.80.241307

PACS number(s): 73.23.-b, 03.65.Yz, 73.43.Cd, 73.43.Lp

I. INTRODUCTION

The recent demonstrations of Mach-Zehnder interferometers (MZIs)¹⁻³ in the integer quantum Hall regime have best illustrated the ballistic and phase coherent character of electronic propagation along the chiral quantum Hall edges over tens of microns. Recently, the development of an on demand single-electron source⁴ has opened the way to fundamental *electron quantum optics* experiments involving single charge excitations such as the electronic Hanbury-Brown and Twiss experiment⁵ or the Hong-Ou-Mandel experiment^{6,7} in which two indistinguishable electrons collide on a beam splitter. But contrary to photons, electrons interact with their electromagnetic environment and with other electrons present in the Fermi sea. This results in relaxation and decoherence of single-electron excitations above the ground state that deeply questions the whole electron quantum optics concept. This has been emphasized in MZI where, despite insensitivity to electron-source time coherence, decoherence along the chiral edges drastically reduces the contrast of interferences.⁸⁻¹³

Recently, energy resolved electronic detection using quantum dots has also been demonstrated,¹⁴ thus opening the way to energy relaxation studies in quantum Hall edge channels. Combining such measurements with the on demand single-electron source will enable experimental testing of the basic problem of quasiparticle relaxation originally considered by Landau in Fermi liquid theory.¹⁵

In this Rapid Communication, we present a full many body solution to this problem in quantum Hall edge channels. To address the above basic issues, we have developed a unified approach of high frequency transport and decoherence and relaxation of coherent single-electron excitations showing the central role of plasmon scattering. This approach opens the way to an in depth understanding of the nature of quasiparticles in various integer quantum Hall edge channels and provides an efficient theoretical framework for electron quantum optics. To illustrate our formalism, we clarify the role of the electronic Fermi sea in single-electron decoherence, explicitly showing the interpolation from a Pauli blockade regime at low energy to a dynamical Coulomb blockade like regime at high energy in which the Fermi sea plays the role of an effective environment.

II. MODEL

Let us consider the specific example of a chiral edge channel capacitively coupled to an external gate of size l connected to a resistance R representing a dissipative external circuit (see Fig. 1). In the integer quantum Hall regime, bosonization expresses the electron creation operator at point x along the edge, $\psi^\dagger(x)$, in terms of a chiral bosonic field $\phi(x)$ as

$$\psi^\dagger(x) = \frac{U^\dagger}{\sqrt{2\pi a}} e^{-i\sqrt{4\pi}\phi(x)}, \quad (1)$$

where a is a short distance cutoff and U^\dagger ensures fermionic anticommutation relations. The bosonic field determines the electron density $n(x) = (\partial_x \phi(x)) / \sqrt{\pi}$. In the presence of an external voltage $U(x, t)$ along the edge, its equation of motion is

$$(\partial_t + v_F \partial_x) \phi(x, t) = \frac{e\sqrt{\pi}}{h} U(x, t), \quad (2)$$

where v_F is the electron Fermi velocity along the edge. Before and after the interaction region delimited by $|x| \leq l/2$,

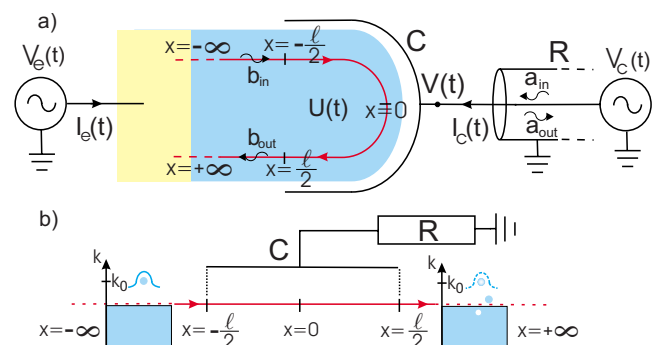


FIG. 1. (Color online) (a) Two terminal device built from an edge channel coupled to an RC circuit. In the interaction area $|x| \leq l/2$, the edge channel (in red) at internal potential $U(t)$ is capacitively coupled to the gate of capacitance C at potential $V(t)$. (b) A single electron is injected in the $x < -l/2$ region and propagates along the edge channel. Interactions within $|x| \leq l/2$ create electron-hole pairs within the edge channel and photons in the RC circuit leading to decoherence.

this chiral field propagates freely and thus defines input (j =in for $x \leq -l/2$) and output (j =out for $x \geq l/2$) plasmon modes,

$$\phi_j(x,t) = \frac{-i}{\sqrt{4\pi}} \int_0^\infty \frac{d\omega}{\sqrt{\omega}} [b_j(\omega) e^{i\omega(x/v_F - t)} - \text{H.c.}] \quad (3)$$

In the interaction area $|x| \leq l/2$, the edge is capacitively coupled to the gate forming a capacitor of capacitance C . Following Prêtre *et al.*,¹⁶ we assume the potential within the edge to be uniform²⁵ and denoted by $U(t)$.¹⁶ The total charge stored within the interaction region

$$Q(t) = -e \int_{-l/2}^{l/2} n(x,t) dx \quad (4)$$

is proportional to the voltage drop between the gate at potential $V(t)$ and the edge channel,

$$C[U(t) - V(t)] = Q(t). \quad (5)$$

Following Refs. 17 and 18, the resistance will be modeled as a quantum transmission line with characteristic impedance $Z=R$. Its degrees of freedom are described by input and output photon modes $a_j(\omega)$ (j =in or out) propagating along the line. The total charge stored within the line is, by neutrality of the RC circuit, equal to $Q(t)$ and expressed in terms of photon modes by

$$Q(t) = \sqrt{\frac{\hbar}{4\pi R}} \int_0^\infty [(a_{\text{in}} + a_{\text{out}})(\omega) e^{-i\omega t} + \text{H.c.}] \frac{d\omega}{\sqrt{\omega}}. \quad (6)$$

The voltage of the gate $V(t)$ is also expressed as

$$V(t) = eR \sqrt{\frac{R_K}{2R}} \int_0^\infty \sqrt{\omega} [i(a_{\text{in}} - a_{\text{out}})(\omega) e^{-i\omega t} + \text{H.c.}] \frac{d\omega}{2\pi}. \quad (7)$$

Using Eqs. (5)–(7), the voltage $U(t)$ can be expressed in terms of the a modes. Solving for the edge equation of motion [Eq. (2)] gives a first linear equation relating the input and output a and b modes. It also expresses the chiral field and total charge within the interaction region in terms of these modes. Using this in Eq. (4) leads to a second linear equation between the input and output a and b modes. This leads to the unitary plasmon to photon scattering matrix $S(\omega) = [S_{\alpha\beta}(\omega)]$ (α, β equal to c for the circuit or e for the edge) at frequency $\omega/2\pi$. In the following $t(\omega) = S_{ee}(\omega)$ will denote the edge plasmon transmission amplitude. As discussed in the case of one-dimensional (nonchiral) wires,¹⁹ it determines the finite frequency admittance. Obviously, this quantity is model dependent but our discussion of its connection with single-electron relaxation is valid in full generality.

III. HIGH FREQUENCY ADMITTANCES

The admittance matrix at frequency ω relates the Fourier component $I_\alpha(\omega)$ of the incoming currents through the various leads α to the voltages $V_\beta(\omega)$ in the linear response regime,

$$I_\alpha(\omega) = \sum_\beta g_{\alpha\beta}(\omega) V_\beta(\omega). \quad (8)$$

In the present case, the input modes can be related to the voltages applied to the edge reservoir and to the RC circuit. First of all, the applied time dependent voltage $V_c(t)$ creates an incoming coherent state within the transmission line characterized by the average value of the incoming a modes,

$$\langle a_{\text{in}}(\omega) \rangle = \frac{-i}{\sqrt{\omega}} \sqrt{\frac{R_K}{2R}} \frac{e V_c(\omega)}{h}. \quad (9)$$

For the edge channel, modeling the reservoir as a uniform time dependent voltage $V_e(t)$ applied from $x = -\infty$ to $x = -l/2$ shows that it injects in the $[-l/2, l/2]$ region a plasmon coherent state fully characterized by the average value of the incoming b modes,²⁰

$$\langle b_{\text{in}}(\omega) \rangle = -\frac{e V_e(\omega)}{h} \frac{1}{\sqrt{\omega}} e^{i\omega l/2v_F}. \quad (10)$$

The finite frequency admittance can then be expressed in terms of the plasmon to photon scattering matrix and reciprocally uniquely determines it. In the present case, due to total screening of charges in the edge channel by the gate, this 2×2 admittance matrix satisfies gauge invariance and charge conservation,¹⁶ $g_{ee} = g_{cc} = -g_{ec} = -g_{ce}$, and is thus determined by a unique admittance,

$$g(\omega) = g_{ee}(\omega) = \frac{e^2}{h} [1 - t(\omega) e^{i\omega l/2v_F}], \quad (11)$$

which is in turn entirely determined by the plasmon transmission amplitude $t(\omega)$. At low frequency and up to second order in ω , the admittance is equivalent to the serial addition of an electrochemical capacitance C_μ and a charge relaxation resistance R_q . Here, C_μ is the series addition of the quantum capacitance $C_q = l/v_F R_K$ (with $R_K = h/e^2$) and the geometric capacitance.¹⁶ The charge relaxation resistance is the sum of the circuit resistance and the half-quantum $h/2e^2$ (Refs. 21 and 22) expected for a single mode conductor.

IV. ELECTRON RELAXATION AND DECOHERENCE

Let us now consider the evolution of a single electron initially prepared [see Fig. 1(b)] in a coherent wave packet. Starting from the zero temperature Fermi sea $|F\rangle$, the many body state with one additional electron in the normalized wave packet $\varphi(x)$ above the Fermi sea is given by $|\varphi, F\rangle = \int \varphi(x) \psi^\dagger(x) |F\rangle dx$.

Single particle spatial coherence and density are described by the off diagonal and diagonal components, respectively, of the single particle reduced density operator $\mathcal{G}_\rho^{(e)}(x, y) = \text{Tr}[\psi(x) \rho \psi^\dagger(y)]$ in which ρ denotes the many body electronic density operator. Going to Fourier space then shows that the single-electron momentum distribution is encoded in the diagonal of the single particle density operator in momentum space.

Before entering the interaction region, the initial many body density operator is given by $\rho_i = |\varphi, F\rangle \langle \varphi, F|$ and then $\mathcal{G}_{\rho_i}^{(e)}(x, y) = \mathcal{G}_F^{(e)}(x, y) + \varphi(y)^* \varphi(x)$ where the first contribution

$\mathcal{G}_F^{(e)}(x, y) = \int n_F(k) e^{ik(x-y)} \frac{dk}{2\pi}$ comes from the Fermi sea ($n_F(k) = \langle c_k^\dagger c_k \rangle_F$) whereas the second one is associated with the coherent single-electron excitation.

Using Eq. (1), the state $|\varphi, F\rangle$ appears as a superposition of incoming plasmon coherent states. Since the interaction region elastically scatters plasmon to photons, the resulting outgoing external circuit+edge quantum state is an entangled superposition of coherent plasmon and photon states. Tracing out over the circuit's degrees of freedom leads to the exact many body electron state after time t such that the initial wave packet has flown through the interacting region,

$$\rho_f = \int dy_+ dy_- \varphi(y_+) \varphi^*(y_-) \mathcal{D}_{\text{ext}}(y_+ - y_-) \times \tilde{\psi}^\dagger(y_+ + v_F t) |F\rangle \times \langle F| \tilde{\psi}(y_- + v_F t), \quad (12)$$

where \mathcal{D}_{ext} is the extrinsic decoherence associated with photon emission into the external circuit,

$$\mathcal{D}_{\text{ext}}(\Delta y) = \exp\left(\int_0^{+\infty} |r(\omega)|^2 (e^{-i(\omega\Delta y/v_F)} - 1) \frac{d\omega}{\omega}\right), \quad (13)$$

where $r(\omega) = S_{ce}(\omega)$ denotes the plasmon to photon scattering amplitude. In Eq. (12), $\tilde{\psi}^\dagger(y)$ is a modified field operator,

$$\tilde{\psi}^\dagger(y) = \frac{U^\dagger}{\sqrt{2\pi a}} \exp\left(\int_0^{+\infty} [t(\omega)b(\omega)e^{i\omega y/v_F} - \text{H.c.}] \frac{d\omega}{\sqrt{\omega}}\right). \quad (14)$$

When $t(\omega)$ is a pure phase linear in ω , $\tilde{\psi}^\dagger(y)$ is a spatially translated fermion field operator. Any other ω dependence of $t(\omega)$ leads to the creation of additional electron-hole pairs that cannot be absorbed in a simple translation.

Relaxation of a single electron can then be discussed by considering an incident energy resolved wave function: $\varphi_{k_0}(x) = e^{ik_0 x}$. The complete momentum distribution consists in the Fermi sea contribution and a change $\delta n_{k_0}(k)$ that can be obtained from single particle coherence $\mathcal{G}_{k_0}^{(e)}$ after interaction with the RC circuit,

$$\int_{\mathbb{R}} e^{-ik(x-y)} \mathcal{G}_{k_0}^{(e)}(x, y) d(x-y) = L n_F(k) + \delta n_{k_0}(k), \quad (15)$$

where L is the total size of the system. The left-hand side can be computed using bosonization thus leading to explicit fully nonperturbative expressions for single-electron relaxation $\delta n_{k_0}(k)$ that will be given in a forthcoming publication.

This detailed analysis shows that, at zero temperature, $\delta n_{k_0}(k)$ has a quasiparticle peak at $k = k_0$ and a nonzero regular part for $-k_0 \leq k < k_0$: $\delta n_{k_0}(k) = Z(k_0) \delta(k - k_0) + \delta n_{k_0}^r(k)$. Finally, the sum rule $Z(k_0) + \int_{-k_0}^{k_0} \delta n_{k_0}^r(k) dk = 1$ reflects particle conservation.

Figure 2(a) presents the regular part $\delta n_{k_0}^r(k)$ as a function of $(k - k_0)l$ at fixed k_0 and Fig. 2(b) shows the weight of the quasiparticle peak $Z(k_0)$ in term of $k_0 l$ for $R = 50 \Omega$ and $l/v_F R_K C = 0.5$. In two limiting regimes, energy relaxation can be described using a single particle relaxation approach by introducing an appropriate effective environment and, at low

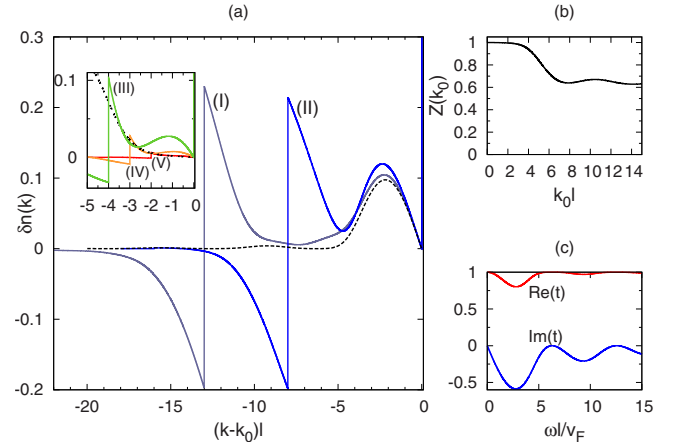


FIG. 2. (Color online) (a) Single electron energy relaxation for $R = 50 \Omega$ and $l/v_F R_K C = 0.5$ plotted against $(k - k_0)l$ for (I) $k_0 l = 13$ and (II) $k_0 l = 8$. The dashed curve corresponds to the single particle result [Eq. (16)] valid at high energies. Inset shows small values of $k_0 l$: (III) 4, (IV) 3, and (V) 2. The dotted line corresponds to the simple relaxation model $\delta n_{k_0}^r(k) = -Z'(k_0 - k)$. (b) Quasiparticle peak $Z(k_0)$. (c) Real and imaginary parts of the plasmon transmission amplitude $t(\omega)$.

energy, taking into account the Pauli exclusion principle.

Close enough to the Fermi surface [see inset of Fig. 2(a)], single-electron relaxation can be described using a simple relaxation model: for $0 \leq k < k_0$, $\delta n_{k_0}^r(k) \approx p(k_0 - k)$, where $p(q)$ can be interpreted as the probability to lose momentum q . The remaining quasiparticle weight $Z(k_0)$ is then related to p by $p(q) = -Z'(q)$. Note that the Fermi sea remains spectator [$\delta n_{k_0}^r(k) = 0$ for $k < 0$] since at low energies $t(\omega)$ is close to 1, thus limiting the creation of electron-hole pairs in the relaxation process. In this regime, energy relaxation is limited by the Pauli exclusion principle. For $R \neq 0$ and at low energy, photon emission is the dominant relaxation mechanism and the inelastic scattering probability $1 - Z(k_0)$, which only depends on the equivalent circuit parameters, scales as $(R_q/R_K - 1/2)(k_0 R_K C_\mu v_F)^2$ at low momentum. Consequently, the quasiparticle is well defined close to the Fermi surface.

At high energies, $\delta n_{k_0}(k)$ splits into two distinct contributions [see, e.g., Fig. 2(a), $k_0 l = 8, 13$]. The first one appears in Fourier space around the Fermi level and corresponds to the electron-hole pairs created by the incident electron. The second one is localized in Fourier space close to k_0 and corresponds to the relaxation of the incoming electron due to photon emission into the transmission line as well as electron-hole pair creation inside the edge channel. In real space, in the limit of very high incident energy, it shows up as an effective decoherence coefficient $\mathcal{D}(x - y)$ acting on the incident wave packet propagated during the time interval $[0, t]$,

$$\varphi(x) \varphi^*(y) \mapsto \varphi(x - v_F t) \varphi^*(y - v_F t) \mathcal{D}(x - y). \quad (16)$$

The decoherence coefficient \mathcal{D} is then a product of the extrinsic contribution [Eq. (13)] and an intrinsic contribution associated with the imprints left within the Fermi sea by the different positions appearing in the single-electron incident wave packet. Finally \mathcal{D} is obtained by substituting $|r(\omega)|^2$ by

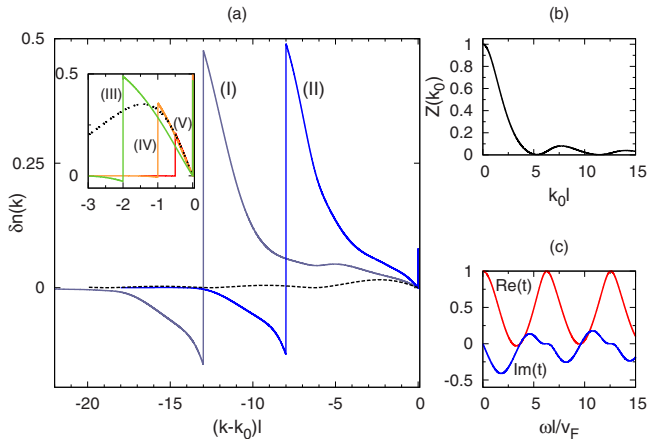


FIG. 3. (Color online) (a) Single electron energy relaxation for $R/R_K=0.5$ and $l/v_F R_K C=0.5$ plotted against $(k-k_0)l$ for (I) $k_0 l=13$ and (II) $k_0 l=8$. The dashed curve corresponds to the single particle result [Eq. (16)] valid at high energies. Inset shows small values of $k_0 l$: (III) 2, (IV) 1, and (V) 0.5. The dotted line corresponds to the simple relaxation model $\delta n_{k_0}^r(k) = -Z'(k_0 - k)$. (b) Quasiparticle peak $Z(k_0)$. (c) Real and imaginary parts of the plasmon transmission amplitude $t(\omega)$.

$2 \operatorname{Re}[1-t(\omega)]$ into Eq. (13). This regime is similar to the dynamical Coulomb blockade,²³ with the Fourier transform of \mathcal{D} playing the role of $P(E)$ [see dashed lines on Figs. 2(a) and 3(a) for the corresponding energy relaxation]. The case of an RC circuit with $R=R_K/2$ exhibits clear deviations from these two limiting approaches in the considered frequency

range [see Fig. 3(a)] thus showing the need of our nonperturbative approach. This arises from the strong plasmon scattering in the relevant frequency range at larger R/R_K [compare Figs. 2(c) and 3(c)]. Note also the faster decay of the quasiparticle peak [compare Figs. 2(b) and 3(b)].

V. CONCLUSION

In this Rapid Communication, we have presented a complete theory of coherent single-electron excitation relaxation in integer quantum Hall edge channels. The scattering between edge plasmonic and environmental modes determines both the finite frequency admittances and relaxation properties of a coherent single-electron excitation. The latter can thus be computed exactly from the finite frequency admittances. This approach can be used to study decoherence and relaxation of single-electron excitations due to interactions within a single edge channel or to interchannel coupling in $\nu=2$ quantum Hall systems. It can also be generalized to fractional quantum Hall edges as well as to the case of nonchiral quantum wires. Finally, relaxation of nonequilibrium distribution functions such as the one created by a biased quantum point contact requires taking into account all Keldysh correlators of currents.²⁴

ACKNOWLEDGMENTS

We warmly thank Ch. Glattli, B. Plaçons, F. Pierre, and P. Roche for useful discussions and remarks.

¹Y. Ji *et al.*, Nature (London) **422**, 415 (2003).

²I. Neder *et al.*, Nature (London) **448**, 333 (2007).

³P. Roulleau, F. Portier, D. C. Glattli, P. Roche, A. Cavanna, G. Faini, U. Gennser, and D. Mailly, Phys. Rev. Lett. **100**, 126802 (2008).

⁴G. Fève *et al.*, Science **316**, 1169 (2007).

⁵R. Hanbury-Brown and R. Twiss, Nature (London) **178**, 1046 (1956).

⁶C. K. Hong, Z. Y. Ou, and L. Mandel, Phys. Rev. Lett. **59**, 2044 (1987).

⁷S. Ol'khovskaya, J. Splettstoesser, M. Moskalets, and M. Büttiker, Phys. Rev. Lett. **101**, 166802 (2008).

⁸G. Seelig and M. Büttiker, Phys. Rev. B **64**, 245313 (2001).

⁹J. T. Chalker, Y. Gefen, and M. Y. Veillette, Phys. Rev. B **76**, 085320 (2007).

¹⁰P. Roulleau, F. Portier, P. Roche, A. Cavanna, G. Faini, U. Gennser, and D. Mailly, Phys. Rev. Lett. **101**, 186803 (2008).

¹¹E. V. Sukhorukov and V. V. Cheianov, Phys. Rev. Lett. **99**, 156801 (2007).

¹²I. P. Levkivskiy and E. V. Sukhorukov, Phys. Rev. B **78**, 045322 (2008).

¹³C. Neuenhahn and F. Marquardt, Phys. Rev. Lett. **102**, 046806

(2009).

¹⁴C. Altimiras *et al.*, Nat. Phys. (to be published).

¹⁵D. Pines and P. Nozières, *The Theory of Quantum Liquids* (Perseus, Cambridge, 1966).

¹⁶A. Prêtre, H. Thomas, and M. Büttiker, Phys. Rev. B **54**, 8130 (1996).

¹⁷B. Yurke and J. S. Denker, Phys. Rev. A **29**, 1419 (1984).

¹⁸G. Fève, P. Degiovanni, and T. Jolicoeur, Phys. Rev. B **77**, 035308 (2008).

¹⁹Y. M. Blanter, F. W. J. Hekking, and M. Büttiker, Phys. Rev. Lett. **81**, 1925 (1998).

²⁰I. Safi, Eur. Phys. J. B **12**, 451 (1999).

²¹M. Büttiker, H. Thomas, and A. Prêtre, Phys. Lett. A **180**, 364 (1993).

²²J. Gabelli *et al.*, Science **313**, 499 (2006).

²³G.-L. Ingold and Y. Nazarov, *Single Charge Tunneling*, NATO Advanced Studies Institute Series B: Physics (Plenum Press, New York, 1992), Vol. 294, pp. 21–107.

²⁴I. Snyman and Y. V. Nazarov, Phys. Rev. B **77**, 165118 (2008).

²⁵This hypothesis is valid for $\omega/2\pi \approx v_F/l$ but the general framework presented here is model independent and thus applies to more realistic models of circuit or edge channel coupling.